Creating a Portfolio of Large-Scale, High-Quality Synthetic Grids: A Case Study

Farnaz Safdarian, Sanjana Kunkolienkar, Jonathan Snodgrass, Adam Birchfield, Thomas J. Overbye
College Station, TX
{fsafdarian, sanjanakunkolienkar, snodgrass, abirchfield, overbye}@tamu.edu

***Abstract*—This paper provides a case study methodology for creating a portfolio of large-scale, high-quality, fictitious but realistic (synthetic) power system models that have been developed based on the publicly available generation and load data of 2019 and then upgraded based on predicted generation and load changes by 2030. As the power grids are constantly changing, instead of creating a case from scratch with future data, we present a strategy to upgrade the same grid, to mimic what is needed for real grid planning. The generators are updated based on proposed generators in the queue from the U.S. Energy Information Administration (EIA) and Electric Reliability Council of Texas (ERCOT) long-term plans. The transmission grid is improved to adjust to these changes. The synthetic grid is created over ERCOT footprint in the U.S. with the capability to represent characteristic features of actual power grids, without revealing any confidential information. This synthetic network model is available online and can be shared freely for research and comparisons in different studies on the future grid with the increased penetration of renewable resources. Geographic data views and validation metrics derived from the North American real grids are used to validate the developed grids.**

***Index Terms*—large scale synthetic grids, power system characteristics, renewable energies, transmission expansion planning**

I. Introduction

One of the main challenges for power system planning and future studies is to have access to future models of the electrical grid. Also, to improve modernized power system models, operation and planning optimization models, to advance algorithms for power system operation and planning in academic studies, distributed energy resources (DER) studies, dynamics, and transient stability studies, there is a strong need for complex and diverse electrical grid data. However, as it is well-known among power system engineers, the electrical grid data is considered critical energy/electricity infrastructure information (CEII) with restricted availability for research and publications.

Historically, IEEE test cases [1] and IEEE Reliability Test System (RTS) cases [2] have been established and widely used in the literature for research and publications. In [3], an estimated model of the European interconnected system is created by utilizing real transmission networks in order to analyze the impacts of cross-border trades. A test system is proposed in [4] based on structural attributes and data from the Independent System Operator (ISO) of New England. MATPOWER Polish systems [5] are also created using the real power system of Poland without many details about the geographical coordinates, while the coordinates of high voltage 400 kV and 220 kV substations were estimated later in [6].

However, there is limited work focusing on the creation and upgrading of complicated and realistic synthetic large-scale power system models using publicly available data that can mimic the full complexity of modern electricity grids for detailed power system studies. To address this issue, Advanced Research Projects Agency-Energy (ARPA-E) started a project and asked for the creation of large-scale synthetic power system networks. Reference [7] provides a summary of one of the related ARPA-E projects.

Over the last decade, a number of larger-scale synthetic grids have been developed [8]–[13]. We have created a portfolio of fictitious but realistic (synthetic) grid models using metrics derived from the actual grids and publicly available generator data from the U.S. Energy Information Administration (EIA) and census data to estimate the load. [11]–[13]

In this paper, the synthetic power system model has been developed and improved based on the publicly available generation and load data in 2019 and the predicted generation upgrades by 2030. Then the transmission grid is improved to adjust to these changes. The synthetic grid is created over the Electric Reliability Council of Texas (ERCOT) footprint in the U.S. with the capability to represent characteristic features of actual power grids, without revealing any CEII. This synthetic network model is available online and can be shared freely for teaching, training, and research purposes and comparisons under the increased penetration of renewable resources. Geographic Data views (GDVs) and validation metrics derived from the North American real grids are used to validate the synthetic grid models.

II. Synthetic ERCOT Case Study based on Real Generator Data

The original synthetic grid that is created over the ERCOT footprint contains 6,717 buses and geographically covers most of Texas. The transmission network is built using the three nominal transmission voltage levels in the actual grid for this

 Presented at the 2024 IEEE Kansas Power and Energy Conference (KPEC), Manhattan, KS, April 2024.
979-8-3503-7240-3/24/$31.00 ©2024 IEEE

TABLE I
2019 SYNTHETIC ERCOT GRID STATISTICS

Number of buses	6,717
Number of substations	4,894
Number of areas	17
Number of transmission lines	7,168
Number of transformers	1,967
Number of phase shifters	2
Number of loads	4,856
Number of generators	731
Number of shunts	634
Load range (GW)	30-80

TABLE II
TYPE AND NUMBER OF GENERATORS IN 2019 SYNTHETIC ERCOT GRID

Fuel Type	Number of Units	MW Capacity Total
Natural Gas	472	56,352
Coal	23	14,407
Nuclear	4	4,960
Wind	153	25,702
Solar	36	2,335
Hydro	22	498
Petroleum	2	53
Battery	2	66
Other	17	960.7
Total	731	104,914

footprint: 345 kV, 138 kV and 69 kV. Table I provides a summary of the important characteristics of this case. Table II shows a summary of EIA-860 generators and unit types in ERCOT footprint. Other fuel types in the Table refers to fuels like wood, biomass and geothermal. The synthetic Texas grid was originally created based on the EIA 860 form of 2019 year generator data [14]. All generators with a capacity larger than 8 MW in the grid are mapped with their corresponding EIA generator based on the EIA plant code and generator ID. The grid with more details is available at [15].

The improvements are made to increase the realness, reliability, and resilience of the grid. The grid is studied over a variety of load and weather scenarios and upgraded to avoid voltage violations and line overloads. The upgrades included adding generator details, cost curves and temporal constraints, creating a variety of load and weather scenarios and contingencies, studying the grid under such scenarios to improve the performance of the grid for significant contingencies and extreme load and weather scenarios, adding reactive power control devices, upgrading transmission lines and partitioning the grid into reserve zones and determine the required real and reactive power reserve [16] to improve the reliability and resiliency of the grid.

To create realistic cost curves, the Continuous Emission Monitoring System (CEMS) heat rate curves [17] are used for thermal generators. All generators are mapped to CEMS data based on factors like fuel type, unit type, geographic location, and their capacity. Fuel costs are used from a variety of publicly available resources including [18] for gas prices, [19] for coal prices, [20] for biomass and the rest of fuels from [21]. Then fuel cost values are benchmarked based on [22]. Cost curves are achieved from fuel prices and heat rates and are validated based on ERCOT's 60-day Security Constraint Economic Dispatch (SCED) [23] report. Also, for renewable generators, nuclear units and other non-thermal generators such as hydro units, references [23] and [24] are used to create cost curves and [25] for validation.

For generator parameters and temporal constraints, we have used publicly available resources to determine realistic values. For startup cost [26] and [27], for shutdown cost [28], for cold startup time [14], for warm startup time [29], for hot startup time [29], for ramp rate up and down [27], for minimum up time [26], [30] and [27], for minimum down time [27] and [30], and for variable operation and maintenance cost [26] and [27] are used. In addition, load offer curves are included for demand response and price responsive demand control studied based on data from [31].

Hourly load time series were generated to create scenarios for solving power flow in different conditions. To generate hourly load time series data at the bus level over the course of years, the authors adopt a methodology outlined in references [32] and [33]. This approach involves utilizing the geographical coordinates of each bus to determine its unique electricity consumption pattern. Subsequently, publicly available time series data for building and facility loads at a granular level are progressively combined to form aggregated load profiles at the bus level. The strategy takes into account the relative proportions of residential, commercial, and industrial loads at each network node, as well as location-specific typical load patterns for buildings and facilities, to construct load profiles at the bus level. Once the bus-load is generated, the total load for each region is computed and adjusted to align with the hourly load data for the respective areas within the ERCOT system. The accuracy of the resulting load profiles is assessed and tuned by comparing them to the ERCOT load data from [34].

Also, weather historical measurements of several years have been collected and used to create a variety of weather scenarios. The strategy for the direct inclusion of weather measurements in the AC OPF calculations is explained in [35]. This method mainly updates the capacity of renewable generators based on the availability of wind and solar resources. The outputs of renewable generators are validated in [36]. The main goal of creating a variety of load and weather scenarios is to study the power system under a variety of extreme scenarios and upgrade the grid in a way to reduce overloaded lines and transformers and any voltage issues to make the system more reliable and resilient.

III. UPGRADING THE SYNTHETIC ERCOT CASE STUDY BASED ON INCREASE IN THE RENEWABLE RESOURCES

A. Upgrading Generators

Since renewable energy resources are being developed quickly, the synthetic ERCOT grid is also modeled for the year 2030 with predicted improvements in renewable resources to facilitate studies and comparisons on the future grids. In the EIA 860 data set, the proposed changes in the generators for

TABLE III
COMPARING GENERATION CAPACITY BY FUEL TYPE FOR SYNTHETIC TEXAS GRID CASE IN 2019 AND 2030

	2019 Capacity (MW)	2030 Capacity (MW)	Difference
Solar	2,335	26,835	24,500
Wind	25,702	55,702	30,000
Natural Gas	56,539	62,434	5,895
Battery	0	1,603	1,603
Coal	14,407	12,966	-1,441

the next three years are mentioned with details of generators' parameters and their proposed locations. In addition, the ERCOT presents a long-term view of the anticipated changes in the grid in a report called Long-Term System Assessment (LTSA) [37]. These data are used to upgrade the synthetic Texas grid based on predictions by year 2030. To determine the type and characteristics of the new generators, the new generators added in 2019 to 2023 from EIA 860 including generator parameters and locations used based on the county that is mentioned in the form, a suitable substation in the same county in the synthetic case is selected and the new generators are added to a new bus with bus numbers that is recognizable in the data. In the cases added to [15] the new buses are starting from 1 while the original bus numbers started from 110001 that the added buses are recognizable. The additional generators from EIA 860 have been added with new generator step-up transformers (GSUs) and the proposed capacities and generator parameters while the IDs of new generators are also recognizable in data [15]. The remaining new generators from 2023 to 2030 are added to the neighboring buses in the same counties with their GSUs to connect to the transmission grid having the similar types and capacities of the originally added generators that are available in form EIA 860. Retirement is also added based on ERCOT LTSA. The main parameters of new generators such as combined cycle plants are approximated based on the fuel type and capacity of the closest existing generator in the current system and the inflation rate is added to the cost curves.

Figure 1 shows the geographical data view (GDV) comparison between the renewable capacities of ERCOT in 2019 and 2030. The generators are slightly moved using auto layout function in the figures to avoid overlapping. All visualizations in this paper are created using PowerWorld [38] software simulator 23. Table III compares the generation capacities of the studied grid in 2019 and 2030.

The main changes by 2030 include the solar plants increase from 2,335 MW capacity in 2019 to 26,835 MW by 2030 with an increase by a factor of 11.5 and the wind turbines will have 30,000 MW increase by 2030 (to 55,702 MW) by a factor of 2.2. The number of generators with the natural gas fuel type also increases but the main part of added units include combined cycle power plants. Retirement is also modeled and two coal units with an overall capacity of 1,441 MW are retired by 2030.

The load is also increased by 20% based on 2019 ERCOT System Planning, Long-Term Hourly Peak Demand and Energy Forecast report.

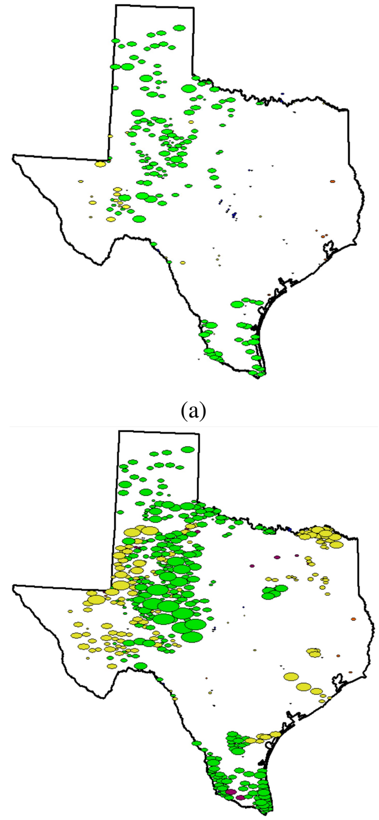

(a)

(b)

Fig. 1. The GDV of renewable generator capacities with the size of ovals proportional to MW capacity, green referring to wind turbines and yellow referring to solar cells in (a) 2019 and (b) 2030 for the synthetic ERCOT grids

B. Upgrading Transmission System

After the new generators are added, the voltage level of buses connected to the large generators is upgraded. This involved adding GSUs and new transformers to connect to the upgraded voltage levels. Then, the transmission grid needs to be upgraded to avoid any line and transformer overloads and create a feasible AC OPF solution.

The overall process was first to split new buses with more than one generator added to them in order to have one bus per generator. Then we added GSUs to the generators and upgraded the voltage levels of buses with added new generators. Transformers were added to connect the new voltage levels to the previous voltages in the same substation.

The transmission system is upgraded in the following steps. First, DC PF (1) is run for all time points in the year 2030 to determine the maximum flow across all of the transmission lines. If the maximum flow exceeds the existing MVA limit then it is flagged as an overloaded line.

$$-[B][\delta] = [P] \tag{1}$$

Next, new conductors are assigned to these flagged lines based on their target MVA limit and voltage level. If upgrading conductors changes the voltage level of a line, the process described above is used to add transformers at the from and to buses if needed. If the overloads are not extreme, it is suggested to upgrade the lines but for extreme overloads a parallel line is added. Finally, the lumped parameter impedance values (resistance R, reactance X, susceptance B) are calculated for the transmission lines and are updated using conductor look-up tables [9].

After updating the transmission lines, the next step is to perform reactive power planning to satisfy bus voltage limits. A modified version of the algorithm described [39] is used. To find an initial AC PF solution, all of the buses are initially modeled as PV buses. This results allow the network operating point to be slowly updated from the DC PF approximation of all buses having 1 pu voltage to a full AC PF solution with loads modeled as PQ buses.

$$P_k = V_k \sum_{n=1}^{N} V_n \left[G_{kn} \cos\left(\delta_k - \delta_n\right) + B_{kn} \sin\left(\delta_k - \delta_n\right)\right] \tag{2}$$

$$Q_k = V_k \sum_{n=1}^{N} V_n \left[G_{kn} \sin\left(\delta_k - \delta_n\right) - B_{kn} \cos\left(\delta_k - \delta_n\right)\right] \tag{3}$$

Using the calculated bus total power net injection from the power flow solution, the non-generator buses modeled as PV buses that have the lowest reactive power (Q) injections are modeled as PQ buses. The ratings of the shunt compensation devices are set to be a higher than the Q injections. The AC PF is run again and these PQ buses are checked for voltage violations. The buses that have exceeded the voltage limits are converted back to PV buses and flagged to add switched shunt compensation. This process is repeated until there is only a certain percentage of PV buses left. Overall, the process is repeated across possible load and weather scenarios for the year 2030. As mentioned in the previous section, the load scenarios are considered the annual 2019 load with a growth factor of 1.2 by 2030 and for weather scenarios, the annual weather measurements from 1970 to 2021 are used as possible weather scenarios in 2030 assuming that weather scenario in each weather can happen as happened in the past. As a result, a power grid is obtained with updated transmission lines and added shunt compensation.

A subsequent for loop facilitates the execution of diverse scenarios. Within this loop, the AC PF is calculated, and a check is performed on the temporarily converted PV buses to ensure their voltage magnitudes fall within the acceptable range of 0.96 per unit (pu) to 1.06 pu. This criterion verifies that the bus's voltage magnitude, derived from its prior status as a PV bus, remains within permissible limits by the addition of a shunt capacitor. Consequently, buses meeting this criterion are flagged with an 'add shunt' designation. The maximum reactive power identified during the AC PF simulations is retained.

TABLE IV
TEXAS SYNTHETIC GRID OVERVIEW IN 2019 AND 2030

	Value in 2019	Value in 2030
Number of buses	6,717	7,132
Number of areas	8	8
Number of transmission lines	7,168	7,223
Number of transformers	1,967	2,332
Number of phase shifters	2	2
Number of loads	4,856	5,095
Number of generators	731	1,058
Number of shunts	634	684

Switched shunts are introduced to buses identified as 'add shunt,' targeting the mid-range of reactive power levels, inductive or capacitive shunts based on the need to inject positive or negative reactive power to the buses to control voltage. If the switched shunt is configured to inject positive reactive power, it is meant to raise the voltage level on the electrical buses and Conversely, if the switched shunt is configured to absorb or provide negative reactive power, it is used to lower the voltage level on the electrical buses. The magnitude of the switched shunts is set at 1.2 times the maximum reactive power recorded during the AC PF simulations to assure the voltage stability of the system during load and weather changes. The buses previously marked with the smallest absolute values of reactive power, as mentioned earlier, are appropriately designated with the PQ flag. This updated grid is available at [15].

IV. VALIDATION

Validating metrics from [40] and [41] are used to compare the main characteristics of the synthetic cases with the real grids. Tables V and VI include general metrics that are created as criteria and extracted from real grids to validate the synthetic grid main characteristics. These Tables compare the main characteristics of synthetic ERCOT grids in 2019 and 2030. Table VII shows the comparisons of topological validating metrics for the synthetic ERCOT grids and real grids. This Table includes topological metrics such as minimum spanning tree (MST) line lengths and Delaunay triangulation distances. Since the topology of the transmission grid is not significantly changed from 2019 to 2030 and mostly the transmission lines are upgraded, the values are similiar for both 2019 and 2030 cases. Table IV shows a comparison of important characteristics of the studied grids in 2019 and 2030.

Additionally, visualization tools such as geographical data view (GDV) [42], voltage contour [43] and wide area visualization of transmission grid [44] were used to visualize the main operation trends of the synthetic grid and real grids over a variety of time horizons and different scenarios and increase the situational awareness of the cases [45]. Figure 2 shows a comparison of net power injection in (a) 2019 and (b) 2030 ERCOT synthetic grids in a high-load and high availability of renewable scenario and the bus voltage contours on the backgound.

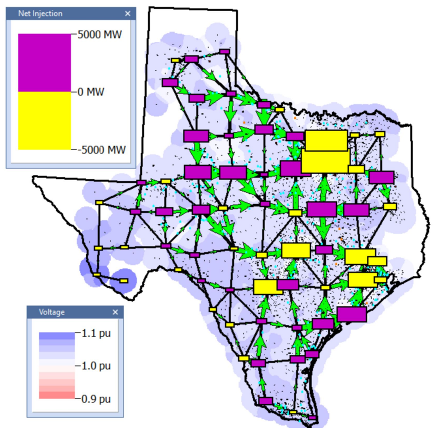

(a)

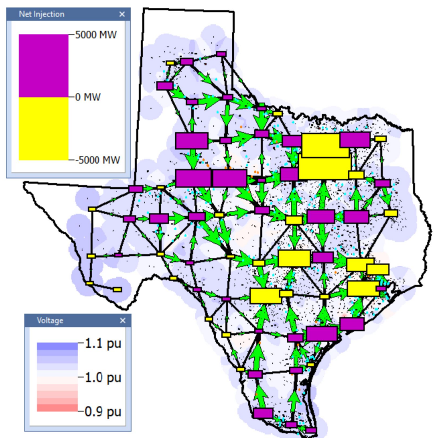

(b)

Fig. 2. The GDV of power flow and net injections of a high load and high renewable scenario with the size of rectangles proportional to MW injection in (a) 2019 and (b) 2030 for the ERCOT synthetic grid

TABLE V
SELECTED VALIDATION METRICS FOR 2019 ERCOT SYNTHETIC GRID (CRITERIA FROM [40] AND [41])

Validation Metric	Criteria	2019 Case
Substations containing buses in kV range	<200 kV, 85-100%	100%
	>201 kV, 5-25%	5.3%
Substations with load	75-90%	90%
Load per bus	Mean 6-18 MW	11.1 MW
Load power factor	Mean 0.93-0.96	0.968
Substations with generators	5-25%	5.9%
Generator MW maximum Capacities	25-200 MW, 40+%	63%
	200+ MW, 2-25%	20%
Committed Generators	60-80%	80%
Shunt capacitors and reactors.	10-25% of subs shunts	11.4%
	30-50% above 200 kV	37.8%

TABLE VI
SELECTED VALIDATION METRICS FOR 2030 ERCOT SYNTHETIC GRID (CRITERIA FROM [40] AND [41])

Validation Metric	Criteria	2030 Case
Substations containing buses in kV range	<200 kV, 85-100%	100%
	>201 kV, 5-25%	5.7%
Substations with load	75-90%	90%
Load per bus	Mean 6-18 MW	12.5 MW
Load power factor	Mean 0.93-0.96	0.968
Substations with generators	5-25%	6.7%
Generator MW maximum Capacities	25-200 MW, 40+%	62%
	200+ MW, 2-25%	25%
Committed Generators	60-80%	80%
Shunt capacitors and reactors.	10-25% of subs shunts	13%
	30-50% above 200 kV	30%

TABLE VII
SELECTED ERCOT TOPOLOGY VALIDATION METRICS (CRITERIA FROM [40] AND [41])

Validation Metric	Criteria	345 kV	138 kV	69 kV
Lines/Substations	1.1-1.4	1.34	1.2	1.2
Lines on MST	40-60%	56.60%	50.6%	48.7%
Distance along Delaunay triangulation	1: 65-85%	85.50%	76.6%	74.3%
	2: 15-25%	12.70%	16.5%	16.7%
	3+: 3-10%	1.70%	6.9%	9%
Total Line Length / MST	1.2-2.2	1.91	1.96	1.8

As it is shown in Figure 2, the areas with higher generation capacity tend to send power to areas with higher load. The comparison of subfigures (a) and (b) shows that added renewable capacity in North East, South and Far Western parts of the grid changes the flow and rectangles from pure absorbing to pure injecting power in these regions. Also, this Figure shows the voltage changes due to the grid updates although the bus voltages in both cases remained from 0.9 pu to 1.1 pu acceptable ERCOT ranges.

V. CONCLUSION

The original synthetic grid that is created over ERCOT footprint contains 6,717 buses and geographically covers most of Texas. The transmission network is built using the three nominal transmission voltage levels that exist in the actual grid for this footprint: 345 kV, 138 kV and 69 kV. The synthetic Texas grid is originally created based on the actual generator data from EIA 860 form of 2019 [14]. The load was originally created based on census data but updated based on [33] to create annual load time series. The improvements are made to increase the realness, reliability, and resilience of the grid.

The 2019 synthetic ERCOT grid is then modified for the year 2030 with predicted improvements in renewable resources to facilitate studies and comparisons on the future grid. The generator updates are based on the EIA 860 proposed changes and ERCOT long-term view of the anticipated changes in a report called Long-Term System Assessment (LTSA) [37]. The load growth is also considered based on LTSA and the transmission grid is upgraded based on AC power flow requirements. The transmission grid upgrades included adding transmission lines and transformers, reactive power control devices, and upgrading transmission lines to avoid operational issues. The synthetic grids are validated based on validation metrics achieved from the North American grids. The grids are also studied over a variety of load and weather scenarios and upgraded to avoid voltage violations and line overloads. Both current and future synthetic network models are available at [15].

VI. Acknowledgements

This work was partially supported through funding provided by the Power Systems Engineering Research Center (PSERC) and partially by Advanced Research Projects Agency–Energy (ARPA-E).

References

[1] [Online]. Available: https://egriddata.org/group/uw-power-systems-test-case-archive

[2] J. Pinheiro, C. Dornellas, M. T. Schilling, A. Melo, and J. Mello, "Probing the new ieee reliability test system (rts-96): Hl-ii assessment," *IEEE Transactions on Power Systems*, vol. 13, no. 1, pp. 171–176, 1998.

[3] Q. Zhou and J. W. Bialek, "Approximate model of european interconnected system as a benchmark system to study effects of cross-border trades," *IEEE Transactions on power systems*, vol. 20, no. 2, pp. 782–788, 2005.

[4] D. Krishnamurthy, W. Li, and L. Tesfatsion, "An 8-zone test system based on iso new england data: Development and application," *IEEE Transactions on Power Systems*, vol. 31, no. 1, pp. 234–246, 2015.

[5] R. D. Zimmerman, C. E. Murillo-Sánchez, and R. J. Thomas, "Matpower: Steady-state operations, planning, and analysis tools for power systems research and education," *IEEE Transactions on power systems*, vol. 26, no. 1, pp. 12–19, 2010.

[6] J. Snodgrass, S. Kunkolienkar, U. Habiba, Y. Liu, M. Stevens, F. Safdarian, T. Overbye, and R. Korab, "Case study of enhancing the matpower polish electric grid," in *2022 IEEE Texas Power and Energy Conference (TPEC)*. IEEE, 2022, pp. 1–6.

[7] F. Safdarian, J. Snodgrass, J. Yeo, A. Birchfield, C. Coffrin, C. Demarco, R. Duthu, S. Elbert, B. Eldridge, T. Elgindy, S. L. Greene, N. Guo, J. Holzer, B. Lesieutre, C. McMillan, H. Mittelmann, R. P. O'Neill, T. J. Overbye, B. Palmintier, A. Tbaileh, P. Van Hentenryck, A. Veeramany, T. W.K. Mak, and J. Wert, "Grid optimization competition on synthetic and industrial power systems," *North American Power Symposium, NAPS*, 2022.

[8] H. Sadeghian and Z. Wang, "Autosyngrid: A matlab-based toolkit for automatic generation of synthetic power grids," *International Journal of Electrical Power & Energy Systems*, vol. 118, p. 105757, 2020.

[9] J. M. Snodgrass, "Tractable algorithms for constructing electric power network models," Ph.D., 2021.

[10] M. Chatzos, M. Tanneau, and P. Van Hentenryck, "Data-driven time series reconstruction for modern power systems research," *Electric Power Systems Research*, vol. 212, p. 108589, 2022.

[11] K. M. Gegner, A. B. Birchfield, T. Xu, K. S. Shetye, and T. J. Overbye, "A methodology for the creation of geographically realistic synthetic power flow models," in *2016 IEEE Power and Energy Conference at Illinois (PECI)*. IEEE, 2016, pp. 1–6.

[12] A. B. Birchfield, T. Xu, K. M. Gegner, K. S. Shetye, and T. J. Overbye, "Grid structural characteristics as validation criteria for synthetic networks," *IEEE Transactions on power systems*, vol. 32, no. 4, pp. 3258–3265, 2016.

[13] F. Safdarian, A. B. Birchfield, K. S. Shetye, and T. J. Overbye, "Additional insights in creating large-scale, high quality synthetic grids: A case study," in *2021 IEEE Kansas Power and Energy Conference (KPEC)*. IEEE, 2021, pp. 1–6.

[14] "Form eia-860," 2019. [Online]. Available: http://www.eia.gov/electricity/data/eia860/index.html.

[15] [Online]. Available: https://electricgrids.engr.tamu.edu/

[16] S. Kunkolienkar, F. Safdarian, J. Snodgrass, and T. J. Overbye, "Creating active and reactive power reserve zones for large-scale electric grids," 2023.

[17] M. Rossol, G. Brinkman, G. Buster, P. Denholm, J. Novacheck, and G. Stephen, "An analysis of thermal plant flexibility using a national generator performance database," *Environmental Science & Technology*, vol. 53, no. 22, pp. 13 486–13 494, 2019.

[18] (2023) "NATURAL GAS". [Online]. Available: https://www.eia.gov/dnav/ng/hist/rngwhhdD.htm

[19] (2023) "Coal markets archive". [Online]. Available: https://www.eia.gov/coal/markets/includes/archive2.phptabs-prices-2

[20] U.S. Environmental Protection Agency. (2019) Biomass Supply Curves in EPA Platform v6. [Online; accessed September 11, 2023]. [Online]. Available: https://www.epa.gov/sites/default/files/2019-03/table_9_biomass_supply_curves_in_epa_platform_v6

[21] (2019) Other Fuels and Fuel Emission Factor Assumptions. [Online; accessed September 11, 2023]. [Online]. Available: https://www.epa.gov/sites/default/files/2019/documents/chapter_9.pdf

[22] (2021) "Weighted Average Cost of Fossil Fuels for the Electric Power Industry". [Online]. Available: https://www.eia.gov/electricity/annual/html/epa_07_04.html

[23] (2023) "ERCOT 60-Day SCED Disclosure Reportsl". [Online]. Available: https://www.ercot.com/mp/data-products/data-product-details?id=NP3-965-ER

[24] (2019) "ERCOT Real Time Co-optimization RTC Tool". [Online]. Available: https://www.ercot.com/mktrules/puctDirectives/rtCoOptimization

[25] (2021) "Average Power Plant Operating Expenses for Major U.S. Investor-Owned Electric Utilities". [Online]. Available: https://www.eia.gov/electricity/annual/html/epa_08_04.html

[26] P. Vaid *et al.*, "Analyses and tabulation of heat rates, unit commitment generator constraint parameter values and emissions estimates of the electricity generators of power plants in texas," Ph.D. dissertation, 2019.

[27] J. B. Garrison, "A grid-level unit commitment assessment of high wind penetration and utilization of compressed air energy storage in ercot," Ph.D. dissertation, 2014.

[28] T. Xu, A. B. Birchfield, K. M. Gegner, K. S. Shetye, and T. J. Overbye, "Application of large-scale synthetic power system models for energy economic studies," 2017.

[29] (2020) "Generator Technical and Cost Parameters". [Online]. Available: https://www.electranet.com.au/wp-content/uploads/projects/2016/11/508986-REP-ElectraNet-Generator-Technical-And-Cost-Parameters-23July2020.pdf

[30] (2019) "Innovation landscape brief: Flexibility in conventional power plants, International Renewable Energy Agency". [Online]. Available: https://www.irena.org

[31] (2023) "NYISO Bid Data". [Online]. Available: http://mis.nyiso.com/public/P-27list.htm

[32] H. Li, A. L. Bornsheuer, T. Xu, A. B. Birchfield, and T. J. Overbye, "Load modeling in synthetic electric grids," in *2018 IEEE Texas Power and Energy Conference (TPEC)*. IEEE, 2018, pp. 1–6.

[33] H. Li, J. H. Yeo, A. L. Bornsheuer, and T. J. Overbye, "The creation and validation of load time series for synthetic electric power systems," *IEEE Transactions on Power Systems*, vol. 36, no. 2, pp. 961–969, 2021.

[34] (2023) "Hourly Load Data Archives". [Online]. Available: https://www.ercot.com/gridinfo/load/load_hist

[35] T. J. Overbye, F. Safdarian, W. Trinh, Z. Mao, J. Snodgrass, and J. H. Yeo, "An Approach for the Direct Inclusion of Weather Information in the Power Flow," *Proc. 56th Hawaii International Conference on System Sciences (HICSS)*, 2023.

[36] J. L. Wert, T. Chen, F. Safdarian, J. Snodgrass, and T. J. Overbye, "Calculation and Validation of Weather-Informed Renewable Generator Capacities in the Identification of Renewable Resource Droughts," in *IEEE PowerTech 2023*, 2023.

[37] "Electric Reliability Council of Texas Long-Term System Assessment". [Online]. Available: http://www.ercot.com/content

[38] [Online]. Available: https://www.powerworld.com//

[39] A. B. Birchfield, T. Xu, and T. J. Overbye, "Power flow convergence and reactive power planning in the creation of large synthetic grids," *IEEE Transactions on Power Systems*, vol. 33, no. 6, pp. 6667–6674, 2018.

[40] A. B. Birchfield, E. Schweitzer, M. H. Athari, T. Xu, T. J. Overbye, A. Scaglione, and Z. Wang, "A metric-based validation process to assess the realism of synthetic power grids," *Energies*, vol. 10, no. 8, p. 1233, 2017.

[41] A. B. Birchfield, "The creation, validation, and application of synthetic power grids," Ph.D. dissertation, 2018.

[42] T. J. Overbye, J. L. Wert, K. S. Shetye, F. Safdarian, and A. B. Birchfield, "The use of geographic data views to help with wide-area electric grid situational awareness," in *2021 IEEE Texas Power and Energy Conference (TPEC)*. IEEE, 2021, pp. 1–6.

[43] J. D. Weber and T. J. Overbye, "Voltage contours for power system visualization," *IEEE Transactions on Power Systems*, vol. 15, no. 1, pp. 404–409, 2000.

[44] T. J. Overbye, J. Wert, K. S. Shetye, F. Safdarian, and A. B. Birchfield, "Delaunay triangulation based wide-area visualization of electric transmission grids," in *2021 IEEE Kansas Power and Energy Conference (KPEC)*. IEEE, 2021, pp. 1–6.

[45] J. L. Wert, F. Safdarian, T. J. Overbye, and D. J. Morrow, "Case study on design considerations for wide-area transmission grid operation visual storytelling," in *2022 IEEE Kansas Power and Energy Conference (KPEC)*. IEEE, 2022, pp. 1–6.